ACS SyntheticBiology

pubs.acs.org/synthbio

Research Article

Discovery of 8-Hydroxyquinoline as a Histamine Receptor 2 Blocker Scaffold

Paola L. Marquez-Gomez,[§] Nicholas S. Kruyer,[§] Sara L. Eisen, Lily R. Torp, Rebecca L. Howie, Elizabeth V. Jones, Stefan France, and Pamela Peralta-Yahya*

Cite This: *ACS Synth. Biol.* 2022, 11, 2820−2828

Read Online

ACCESS | Metrics & More | Article Recommendations | Supporting Information

ABSTRACT: Histamine receptor 2 (HR_{H2}) activation in the stomach results in gastric acid secretion, and HR_{H2} blockers are used for the treatment of peptidic ulcers and acid reflux. Over-the-counter HR_{H2} blockers carry a five-membered aromatic heterocycle, with two of them additionally carrying a tertiary amine that decomposes to N-nitrosodimethylamine, a human carcinogen. To discover a novel HR_{H2} blocker scaffold to serve in the development of next-generation HR_{H2} blockers, we developed an HR_{H2}-based sensor in yeast by linking human HR_{H2} activation to cell luminescence. We used the HR_{H2}-based sensor to screen a 403-member anti-infection chemical library and identified three HR_{H2} blockers, chlorquinaldol, chloroxine, and broxyquinoline, all sharing an 8-hydroxyquinoline scaffold, which is not found among known HR_{H2} antagonists. Critically, we validate their HR_{H2}-blocking ability in mammalian cells. Molecular docking suggests that the HR_{H2} blockers bind the histamine binding pocket and structure−activity data point toward these blockers acting as competitive antagonists. Chloroxine and broxyquinoline are antimicrobials that can be found in the gastrointestinal tract at concentrations that would block HR_{H2}, thus likely modulating gastric acid secretion. Taken together, this work demonstrates the utility of GPCR-based sensors for rapid drug discovery applications, identifies a novel HR_{H2} blocker scaffold, and provides further evidence that antimicrobials not only target the human microbiota but also the human host.

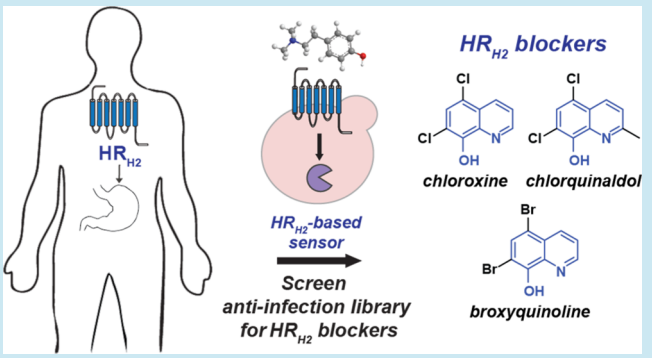

INTRODUCTION

The histamine receptor 2 (HR_{H2}) is expressed in gastric parietal cells, and activation by histamine produced by enterochromaffin-like cells results in gastric acid secretion.[1] Gastric acid causes heartburn and acid reflux in 30% of the US population,[2] with these issues manifesting chronically as gastroesophageal reflux disease (GERD) for 18−27% of the population.[3]

HR_{H2} antagonists, such as ranitidine (Zantac), cimetidine (Tagamet), famotidine (Pepcid), and nizatidine (Mylan), are used as over-the-counter medications to reduce gastric acid secretion in the treatment of peptidic ulcers and acid reflux. All four HR_{H2} blockers are composed of a five-membered aromatic heterocycle. Two of them, ranitidine and nizatidine, additionally contain a tertiary amine that decomposes to N-nitrosodimethylamine,[4,5] a human carcinogen, which has led to the recall of these drugs from the market[6] (Figure 1A). The limited structural diversity among HR_{H2} blockers in clinical use is likely due to the drug discovery approach. Cimetidine was identified in the 1970s by synthesizing a series of histamine analogues and testing their effectiveness for blocking HR_{H2}.[7] Ranitidine, famotidine, and nizatidine are variants of cimetidine. A new HR_{H2} blocker scaffold could aid in the structure−function understanding of HR_{H2} and serve as a starting point to develop next-generation treatment for peptidic ulcers and acid reflux.

A high-throughput drug discovery approach could be applied to identify novel HR_{H2} blocker scaffolds. Such an approach requires access to a robust and rapid HR_{H2} blocking assay.[8] While activation of HR_{H2} leads to cAMP accumulation in CHO cells[9] and transcriptional upregulation of anti-inflammatory proteins in macrophages,[10] mammalian-based assays require 1−2 weeks from cell culture to assay results. The extended time length required for the current HR_{H2} activation assay, coupled to its potentially difficult adaptation to high-throughput screening, limits the discovery of new HR_{H2} blocker scaffolds.

Previously, we have engineered G-protein-coupled receptor (GPCR)-based sensors in yeast by expressing human GPCRs

Received: April 19, 2022
Published: August 5, 2022

https://doi.org/10.1021/acssynbio.2c00205
ACS Synth. Biol. 2022, 11, 2820−2828

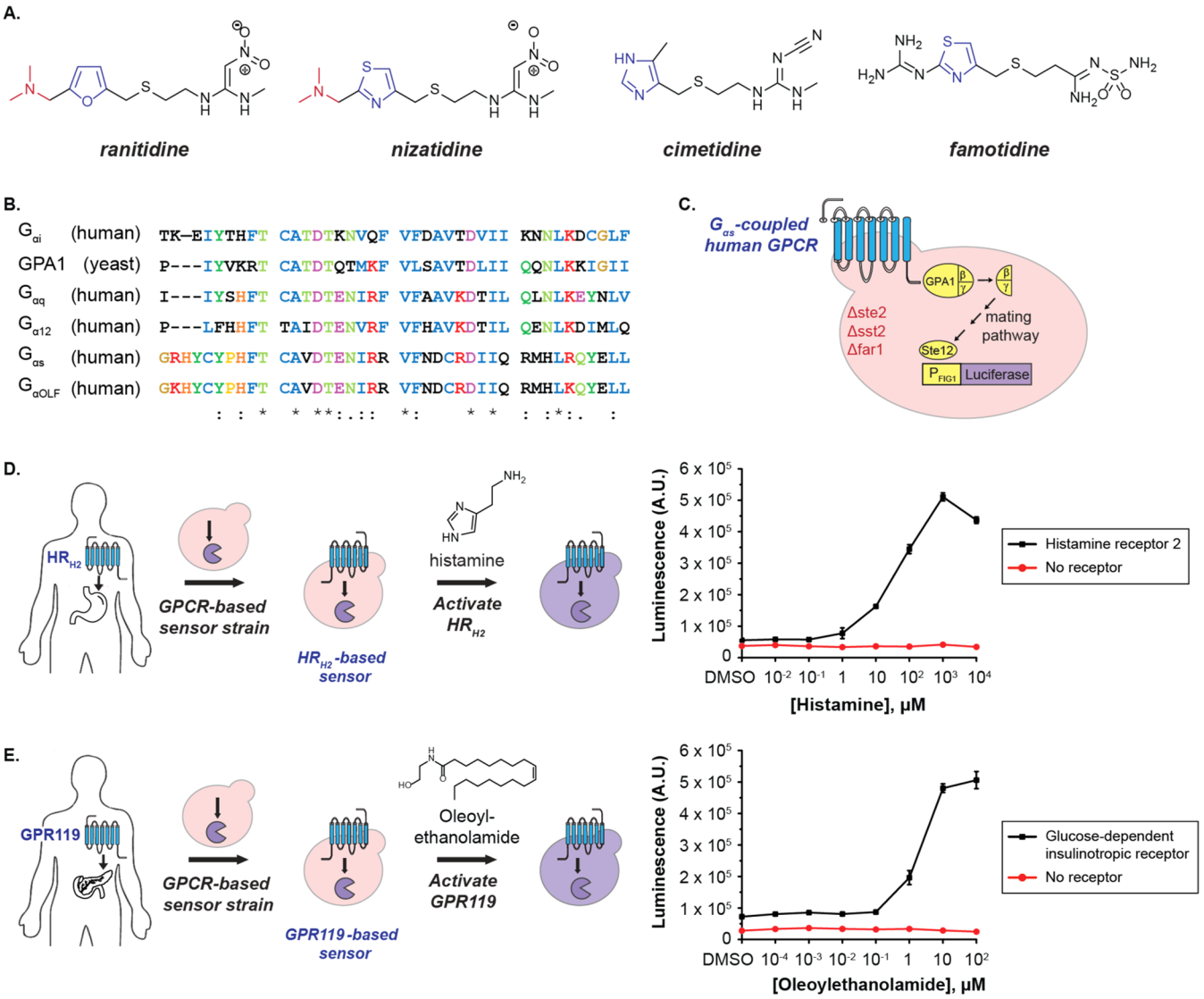

Figure 1. Development of $G_{\alpha s}$-coupled GPCR-based sensors. (A) Over-the-counter HR_{H2} blockers: ranitidine (Zantac), cimetidine (Tagamet), famotidine (Pepcid), and nizatidine (Mylan). All blockers share a five-membered aromatic heterocycle (blue). Ranitidine and nizatidine contain a tertiary amine (red) that decomposes to *N*-nitrosodimethylamine, a human carcinogen. (B) Sequence alignment of the five human G_{α} subunits and the yeast G_{α} (GPA1). Uniprot codes: $G_{\alpha i}$ (P63096), GPA1 (P08539), $G_{\alpha q}$ (P50148), $G_{\alpha 12}$ (Q03113), $G_{\alpha s}$ (P63092), and $G_{\alpha olf}$ (P38405). (C) Schematic of the GPCR-based sensor in yeast. Activation of the GPCR (blue) on the yeast cell surface couples to GPA1 (yellow) that activates the yeast mating pathway ultimately resulting in luciferase expression (purple). (D) Dose−response curve of the HR_{H2}-based sensor with histamine. (E) Dose−response curve of the glucose-dependent insulinotropic receptor (GPR119)-based sensor with oleoylethanolamide. All experiments were performed in triplicate. Shown are the mean and standard deviation.

on the cell surface and coupling their activation to the yeast machinery, ultimately resulting in cell fluorescence[11] or luminescence.[12] By coupling human GPCRs to the yeast G_{α} subunit, GPA1, we have generated sensors using olfactory receptors,[13] which natively couple to $G_{\alpha olf}$ in olfactory neurons, and the serotonin receptor 4 (5-HTR_4),[12,14] which couples to $G_{\alpha s}$ in mammalian cells. Given that HR_{H2} couples to $G_{\alpha s}$, we hypothesized that it would also couple to the yeast machinery via GPA1.

Here, we engineer an HR_{H2}-based sensor in yeast to aid in the discovery of a new HR_{H2} blocker scaffold. Hypothesizing that $G_{\alpha s}$-coupled human GPCRs can couple to the yeast machinery via GPA1 for the generation of sensors, we set out to couple HR_{H2}, a glucose-dependent insulinotropic receptor (GPR119), and a bile acid receptor (GPBAR1) to the yeast machinery. HR_{H2} and GPR119 coupled successfully to the yeast machinery; however, GPBAR1 did not. Next, we confirmed that the HR_{H2}-based sensor could detect the known HR_{H2} blocker famotidine. Then, we used the HR_{H2}-based sensor to screen a 403-member anti-infection chemical library for antimicrobial compounds that block HR_{H2} activation. We identified three antimicrobial agents, chloroxine, chlorquinaldol, and broxyquinoline, to act as HR_{H2} blockers in yeast. Interestingly, these compounds share an 8-hydroxyquinoline scaffold, which is not found among known HR_{H2} antagonists. Therefore, we validate chloroxine, chlorquinaldol, and broxyquinoline to also block HR_{H2} in mammalian cells. Molecular docking suggests the HR_{H2} blockers bind the HR_{H2} orthosteric site and initial structure−activity data suggest that HR_{H2} blockers act as competitive antagonists. The identification of 8-hydroxyquinoline as an HR_{H2} blocking scaffold

https://doi.org/10.1021/acssynbio.2c00205
ACS Synth. Biol. 2022, 11, 2820−2828

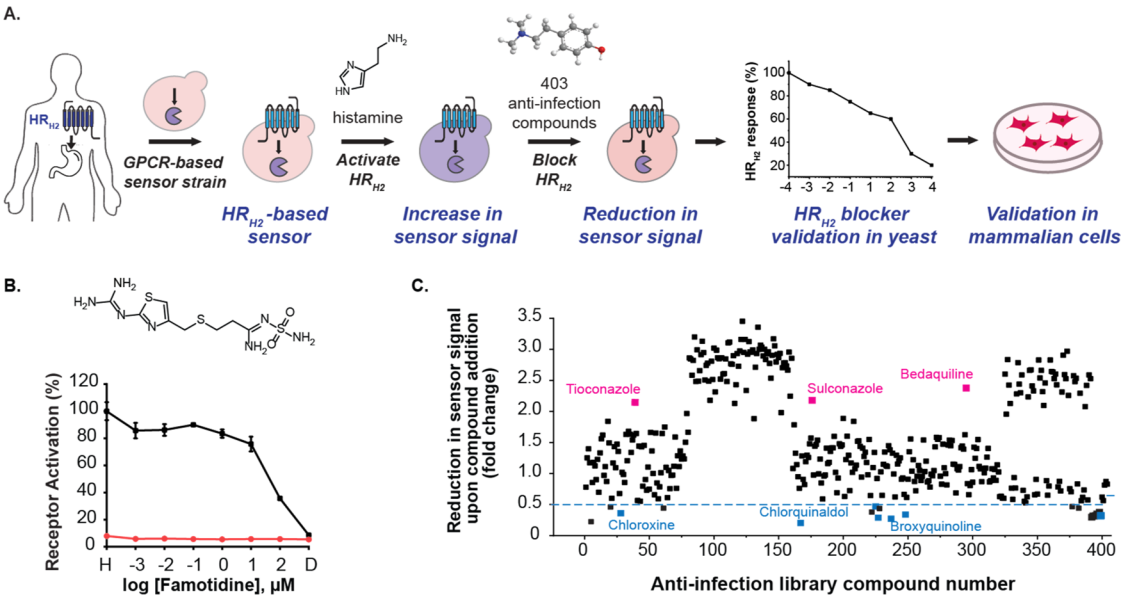

Figure 2. Applying the HR_{H2}-based sensor for HR_{H2} blocker discovery. (A) Workflow for the discovery of HR_{H2} blockers. The HR_{H2}-based sensor in yeast is activated by histamine. HR_{H2} blockers are identified by activating the sensor with histamine and screening a 403-member anti-infection chemical library for a decrease in sensor signal. The HR_{H2} blocker hits are validated in yeast and mammalian cells. (B) Validation of the HR_{H2}-based sensor in yeast using the known HR_{H2} blocker famotidine. Black line: HR_{H2}-based sensor in the presence of histamine (1 mM) and famotidine (10^{-3}–10^{2} μM). Red line: control strain, i.e., yeast sensor expressing an empty plasmid instead of HR_{H2} under the same conditions. "H" is the sensor signal in the presence of 1 mM histamine only. "D" is the sensor signal in the presence of the carrier solvent DMSO only. All experiments were performed in triplicate. Shown are the mean and standard deviation. (C) Screening of 403-member anti-infection chemical library for the identification of HR_{H2} blockers. Blue squares: chemicals that show >50% reduction in HR_{H2}-based sensor signal (dashed line 0.5). Pink squares: sample compounds that show increased fluorescence.

has the potential to open the doors to the synthesis of next-generation HR_{H2} blockers.

RESULTS AND DISCUSSION

Construction of $G_{\alpha s}$-Based Sensors in Yeast. The C-terminus of the G_{α} subunit plays a critical role in coupling GPCRs to the signaling pathway.[15] A sequence alignment of five human G_{α} subtypes revealed that the C-termini of $G_{\alpha s}$ and $G_{\alpha olf}$ are highly conserved, with a 95% amino acid identity over the same range (Figure 1B). Although least similar to GPA1 (22.5% identity over the final 40 C-terminal residues), both $G_{\alpha s}$- and $G_{\alpha olf}$-coupled GPCRs have been successfully connected to the yeast machinery via GPA1.[11,14] This is unsurprising as $G_{\alpha s}$-coupled receptors are known to show more promiscuous G-protein coupling.[15]

To determine the generality of building $G_{\alpha s}$-coupled GPCR-based sensors in yeast, we swapped 5-HTR_4 from the previously developed 5-HTR_4-based sensor[12] with three mammalian $G_{\alpha s}$-coupled GPCRs: HR_{H2}, GPR119, and GPBAR1 (Figure 1C). GPR119 is expressed in pancreatic β-cells, which secrete insulin upon activation by oleoylethanolamide (OEA), making GPR119 a pharmaceutical target for new antidiabetic drugs.[16] Of note, GPR119 has been previously coupled to the yeast machinery via a GPA1-$G_{\alpha s}$ chimera.[17] GPBAR1 is overexpressed in macrophages and when activated reduces the expression of inflammatory genes.[18]

HR_{H2} and GPR119 couple to the yeast machinery via GPA1. The HR_{H2}-based sensor results in a 9-fold increase in signal after activation upon the addition of 1 mM histamine (Figure 1D). The GPR119-based sensor has a 7-fold increase in signal after activation upon the addition of 100 μM OEA (Figure 1E). Histamine and OEA show limited activation of the sensor control strain, where the vector expressing the receptor has been swapped with an empty vector, confirming that the sensor activation is GPCR-dependent. GPBAR1 did not couple to GPA1 (Supporting Figure 1), underscoring the fact that GPCR-G_{α} coupling is a complex multisurface process.[15] Of note, because the GPCR-based sensors are plasmid-based, we screened six distinct colonies to identify optimal biosensor response, with ≥50% of colonies giving robust agonist response. The difference in response is attributed to the fact that the GPCRs are expressed from a multicopy plasmid, leading to a different number of GPCRs trafficking to the membrane in each strain (Supporting Figure 2).

The HR_{H2}-based sensor in yeast could be used to identify HR_{H2} blockers by first activating the sensor with histamine followed by blocker addition. HR_{H2} blocker hits would then be validated in yeast, and ultimately in mammalian cells (Figure 2A). First, the HR_{H2}-based sensor was validated by detecting famotidine, a known HR_{H2} blocker (Figure 2B). Next, the HR_{H2}-based sensor was used to screen a 403-member anti-infection chemical library for HR_{H2} blockers (Figure 2C). Twenty-one compounds reduced histamine-activated HR_{H2} signal by ≥50% (<0.5-fold activation compared to histamine-only signal). Some of the compounds that resulted in an increase in sensor luminescence turned out to be antifungal agents, including tioconazole, sulconazole, and bedaquiline.[19] The increase in the luminescence of tioconazole was corroborated via a dose–response curve (Supporting Figure 3). Thus, increased sensor luminescence was likely nonspecific.

Validation of HR_{H2} Blocker Hits in Yeast. To eliminate false positives, we run dose–response curves of the 21 HR_{H2} blocker hits (Supporting Figure 4). Seven of the 21 hits: chlorquinaldol, chloroxine, broxyquinoline, closantel, octeni-

https://doi.org/10.1021/acssynbio.2c00205
ACS Synth. Biol. 2022, 11, 2820–2828

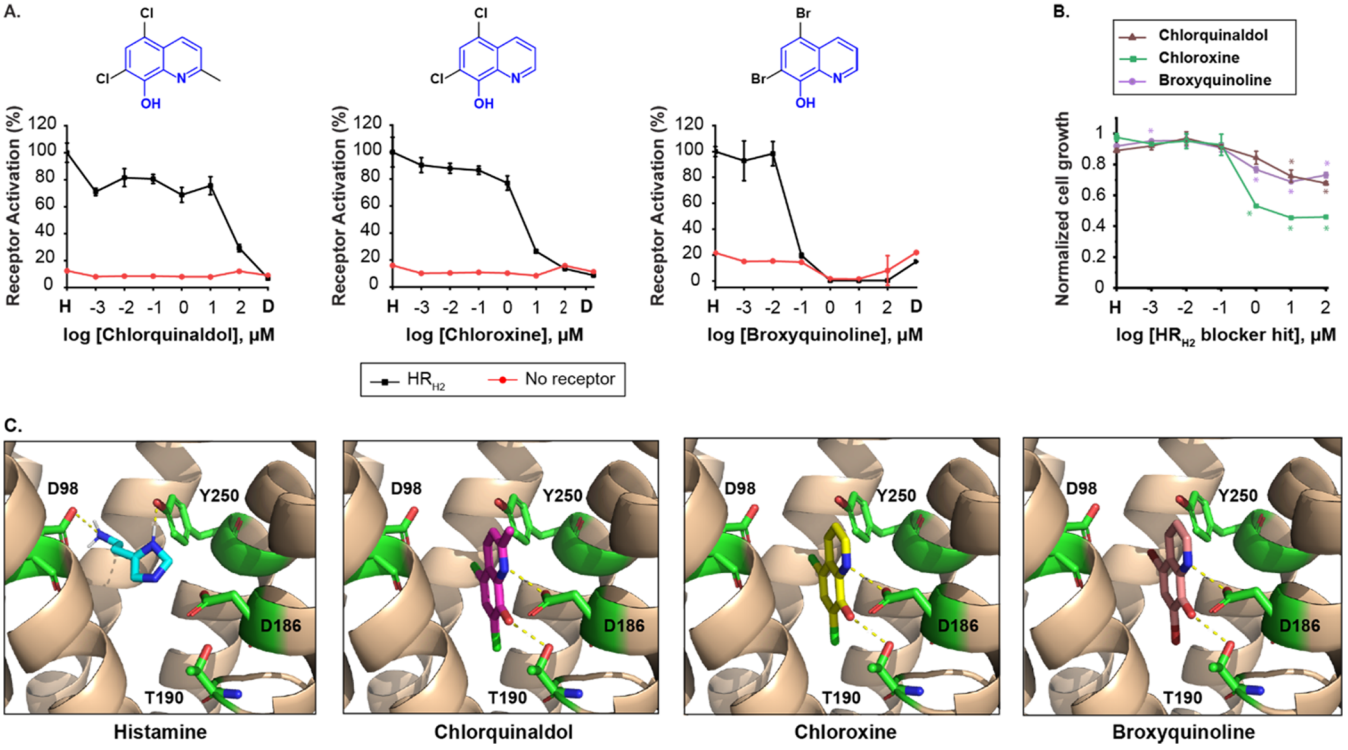

Figure 3. Validation of the HR_{H2} blocker hits from the anti-infection library in yeast. (A) Dose−response curve of the HR_{H2}-based sensor with chlorquinaldol, chloroxine, and broxyquinoline. Black line: HR_{H2}-based sensor in the presence of histamine (1 mM) and HR_{H2} blocker hits (10^{-3}−10^{2} μM). Red line: Control strain, i.e., yeast sensor expressing an empty plasmid instead of HR_{H2} under the same conditions. "H" is the sensor signal in the presence of histamine (1 mM) only. "D" is the sensor signal in the presence of the carrier solvent DMSO only. The 8-hydroxyquinoline scaffold is in blue. Dose−response curves of closantel, octenidine, cetylpyridinium, and enroflaxacin can be found in Supporting Figure 5. (B) Toxicity assessment of chlorquinaldol, chloroxine, and broxyquinoline to yeast; * represents statistically significantly different cell growth ($P < 0.005$). All experiments were performed in triplicate. Shown are the mean and standard deviation. (C) Docking of histamine (blue), chlorquinaldol (magenta), chloroxine (yellow), and broxyquinoline (pink) in a model of the HR_{H2} receptor (gray) showing with key residues D98, Y250, D186, and T190 (green) and electrostatic interactions (dotted yellow lines).

dine, cetylpyridinium, and enrofloxacin lowered the histamine-activated HR_{H2}-based sensor signal in a dose-dependent manner. To ensure that the signal observed was GPCR-dependent, we compared the decrease in luminescence signal from the histamine-activated HR_{H2}-based sensor to that of a control strain carrying an empty vector instead of the HR_{H2} in the presence of the 7 HR_{H2} blocker hits (Figure 3A and Supporting Figure 5). Closantel and enroflaxin failed to lower histamine-activated HR_{H2}-based sensor signal. Cetylpyridinium, and octenidine, lowered histamine-activated HR_{H2}-based sensor signal in a dose-dependent manner. However, we discarded cetylpyridinium and octenidine as *bona fide* HR_{H2} blockers as they are charged compounds with long chain hydrocarbon tails, which could embed themselves in the yeast membrane causing nonspecific cell toxicity, resulting in a reduction in the luminescent signal. Indeed, both compounds have been shown to be toxic to *Saccharomyces cerevisiae*.[20,21] Chlorquinaldol, chloroxine, and broxyquinoline all share an 8-hydroxyquinoline scaffold, which has not been previously linked to HR_{H2} blockers[22] (Figure 3A). Thinking that the 8-hydroxyquinoline scaffold may be interfering with DNA replication or transcription, thus imparting toxicity to yeast, we measured their toxicity to yeast. For all three compounds, some reduction in cell growth can be observed above 0.1 μM. Chloroxine leads to a 50% reduction in cell growth at more than 1 μM. Chlorquinaldol and broxyquinoline have lower cell toxicity, leading to a 20% reduction in cell growth reduction at more than 100 μM (Figure 3B).

Insight into 8-Hydroxyquinoline Binding. The 8-hydroxyquinoline scaffold is intriguing as it lacks the basic amine group commonly found among aminergic GPCR antagonists.[23] To assess how the 8-hydroxyquinoline scaffold may be binding to HR_{H2}, we docked chlorquinaldol, chloroxine, and broxyquinoline to the AlphaFold model of HR_{H2}[24,25] as there is no crystal structure available for HR_{H2}. Previously, Asp98, Asp186, and Thr190 have been experimentally determined to be important for HR_{H2} histamine binding;[26] thus, those residues were used to define the HR_{H2} orthosteric site. As shown in Figure 3C, the model suggests that the amino group of histamine forms a hydrogen bond with Asp98 (2.9 Å), which is consistent with previous experimental studies.[26] The protonated nitrogen in the imidazole ring forms a hydrogen bond with Tyr250 (2.9 Å), which is consistent with previous molecular dynamics simulations that involve Tyr250 in HR_{H2} agonist binding.[27] Confident that the model was docking histamine at the correct location, we docked chlorquinaldol, chloroxine, and broxyquinoline. Interestingly, the three 8-hydroxyquinoline antagonists bound slightly lower in the binding pocket. The hydroxyl group makes electrostatic interactions with Thr190 (2.7 Å), while the protonated nitrogen in the quinoline ring makes electrostatic interactions with Asp186 (2.7 Å) rather than the canonical Asp98. Taken together, these docking studies suggest that the 8-hydrox-

https://doi.org/10.1021/acssynbio.2c00205
ACS Synth. Biol. 2022, 11, 2820−2828

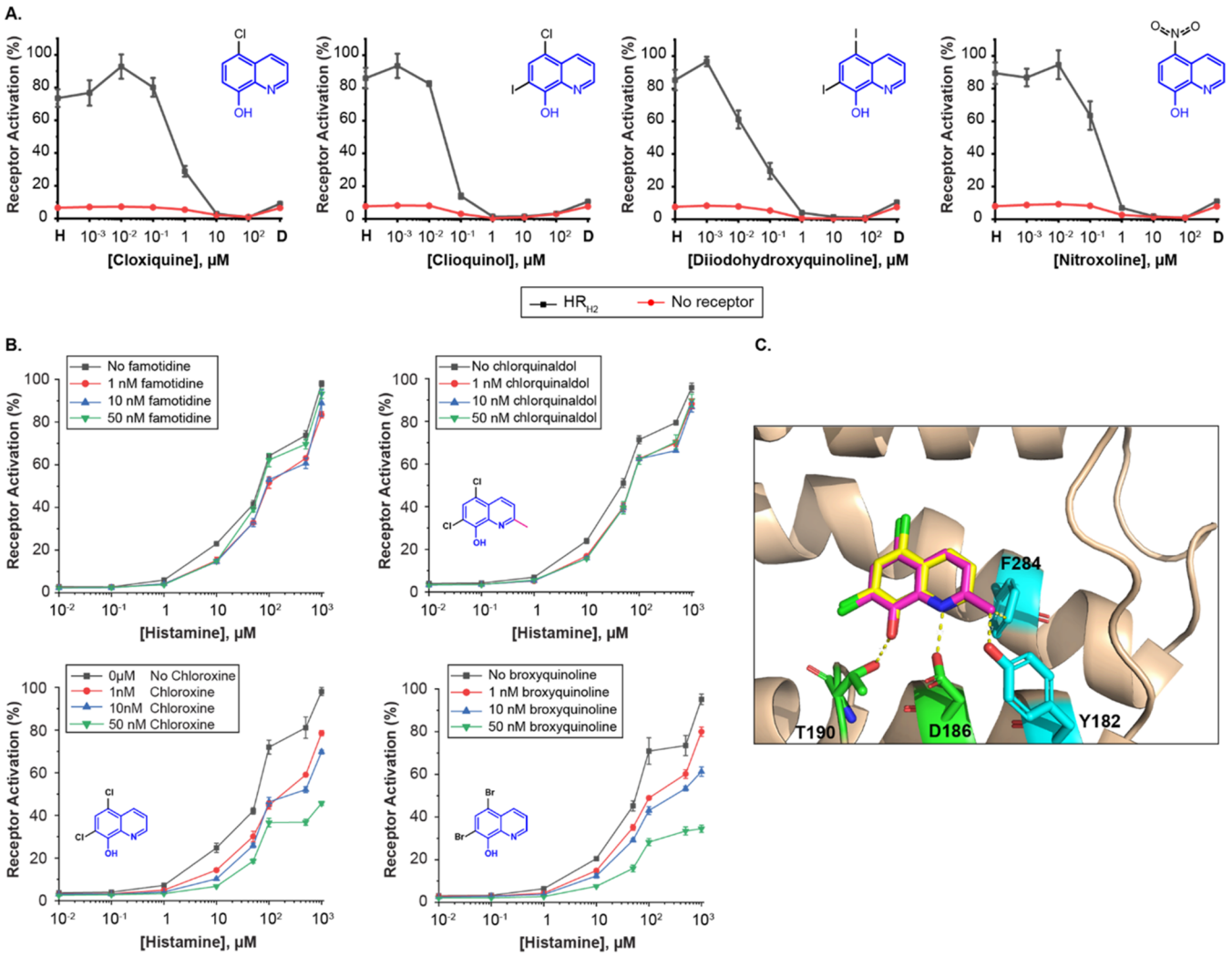

Figure 4. 8-Hydroxyquinoline as a general HR$_{H2}$ blocker scaffold. (A) HR$_{H2}$-dependent decrease in sensor signal in the presence of other 8-hydroxyquinoline-containing compounds found in the anti-infection library. Black line: HR$_{H2}$-based sensor in the presence of histamine (1 mM) and 8-hydroxyquinoline-containing compounds (10^{-3}–10^{2} μM). Red line: control strain, i.e., yeast sensor strain expressing an empty plasmid instead of HR$_{H2}$ under the same conditions. "H" is the sensor signal in the presence of histamine (1 mM) only. "D" is the sensor signal in the presence of the carrier solvent DMSO only. (B) Dose–response curves of the HR$_{H2}$-based sensor in the presence of various concentrations of histamine and famotidine, chlorquinaldol, chloroxine, and broxyquinoline. The 8-hydroxyquinoline scaffold is in blue. The C2 methyl in chlorquinaldol is in pink. All experiments were performed in triplicate. Shown are the mean and standard deviation. (C) Docking overlay of chlorquinaldol (magenta) and chloroxine (yellow) on HR$_{H2}$. Residues T190 and D186 (green) have electrostatic interactions with 8-hydroxyquinoline. Residues F254 and Y182 (cyan) are in close proximity to C_2 methyl in chlorquinaldol.

yquinoline-based HR$_{H2}$ blockers bind the HR$_{H2}$ orthosteric site, and thus are likely competitive antagonists.

8-Hydroxyquinoline as a General HR$_{H2}$-Blocker Scaffold. To assess the generality of 8-hydroxyquinoline scaffold to block HR$_{H2}$, we scanned the anti-infection library for compounds containing 8-hydroxyquinoline that may have shown as false negative in our original screen. Cloxiquine, clioquinol, diiodohydroxyquinoline, and nitroxoline were the most similar compounds, all of them carrying the 8-hydroxyquinoline core, and varying only in the number and identity of the halogen groups on the phenyl ring. Dose–response curves of cloxiquine, clioquinol, diiodohydroxyquinoline, and nitroxoline decrease the signal from the histamine-activated HR$_{H2}$-based sensor in a GPCR-dependent and dose-dependent manner (Figure 4A).

Insight into the 8-Hydroxyquinoline Mode of Action. Chlorquinaldol only differs from chloroxine by a methyl group at C_2. In broxyquinoline, the chlorine atoms from chloroxine have been swapped with bromine. To gain further insight into the role of the C_2 position and the increasing size of the halogen groups at positions C_5 and C_7, we run dose–response curves varying both blocker and histamine concentrations. As shown in Figure 4B, famotidine, a known reversible competitive antagonist, can be displaced by increasing concentration of histamine to recover full HR$_{H2}$ receptor activation. A similar behavior is observed with chlorquinaldol. Chloroxine and broxyquinoline, however, cannot be competed out with increasing histamine concentration, hinting at a potential irreversible competitive antagonist behavior. An overlay of docked chlorquinaldol and chloroxine on HR$_{H2}$ shows that the C_2 methyl is in a very crowded region, with Tyr182 and Phe254 approximately 3 Å away (Figure 4C), which may facilitate chlorquinaldol displacement by histamine. Taken together, the data suggest that the methyl group at C_2 in

https://doi.org/10.1021/acssynbio.2c00205
ACS Synth. Biol. 2022, 11, 2820–2828

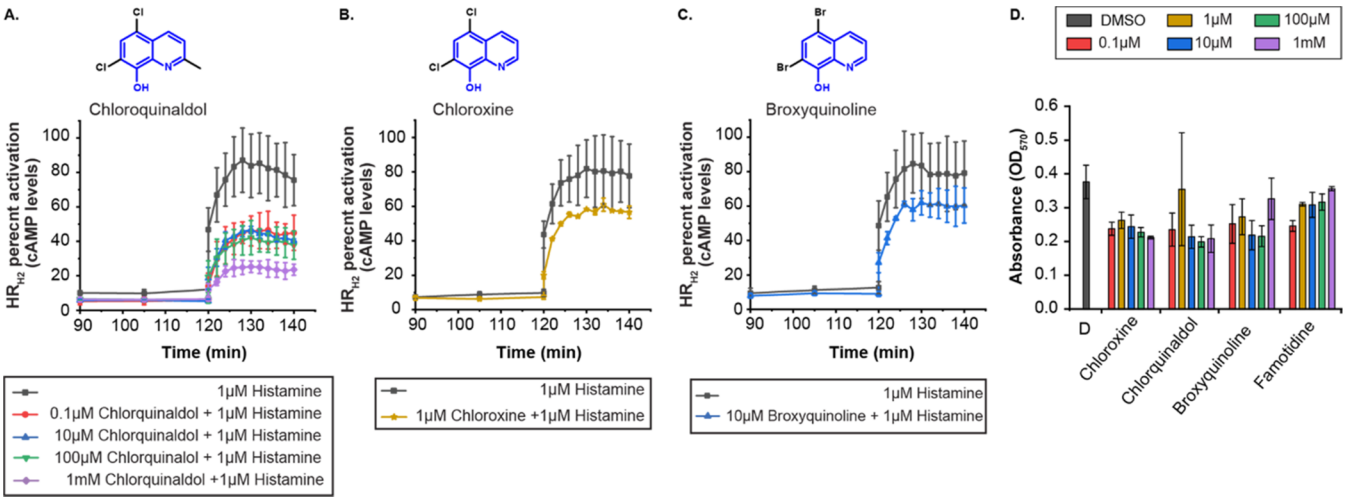

Figure 5. Validation of the HR_{H2} blocker hits in mammalian cells. (A–C) Dose–response curves of mammalian cells (HEK293T) cells co-transfected with HR_{H2} and cAMP sensor in the presence of histamine (1 μM) and various concentrations of (A) chlorquinaldol, (B) chloroxine, and (C) broxyquinoline. (A, C) Average and standard deviation of three independent transformants. (B) Average and standard deviation of three independent transformants in the case of "1 μM histamine" and two independent transformants in the case of "1 μM chloroxine and 1 μM histamine". (D) Cell viability assessment of mammalian cells in the presence of chloriquinaldol, chloroxine, broxyquinoline, famotidine, or the carrier solvent DMSO using an MTT cell proliferation assay.

the 8-hydroxyquinoline scaffold may be sufficient to alter the antagonism mechanism.

Validation of HR_{H2} Blocker Hits in Mammalian Cells. As chlorquinaldol, chloroxine, and broxyquinoline were identified in yeast, we validated their ability to block HR_{H2} in mammalian cells (Figure 5). In mammalian cells, HR_{H2} couples to $G_{\alpha s}$, and the addition of histamine results in an increase in cAMP levels. We expressed HR_{H2} in HEK293T cells and measured the decrease in cAMP levels of cells in the presence of histamine only, and histamine with different concentrations of chlorquinaldol, chloroxine, or broxyquinoline. As shown in Figure 5A, the addition of 1 μM histamine and 0.1 μM or more than 10 μM chlorquinaldol significantly reduces cAMP levels compared to cells activated with 1 μm histamine. At 1 μM, chlorquinaldol seems to also block HR_{H2}, albeit the data were too noisy to draw any conclusions (Supporting Figure 6). The noisiness of the data can be explained by the fact that the cells were transiently expressed with HR_{H2} and the cAMP sensor. In the presence of 1 μM histamine and either 10 μM broxyquinoline or 1 μM chloroxine, a decrease in cAMP levels was also observed (Figure 5B,C). Importantly, none of the HR_{H2} blockers showed major toxicity to mammalian cells up to 1 mM concentration as measured using an MTT cell proliferation assay for cell viability (Figure 5D). Indeed, the toxicity elicited by the three validated HR_{H2} blocker hits is comparable to that elicited by the known HR_{H2} blocker famotidine. Finally, we corroborated the identity of the chlorquinaldol, chloroxine, and broxyquinoline via proton and carbon nuclear magnetic resonance (Supporting Figures 7–12)

Biological Relevance of Newly Identified HR_{H2}-Blockers. HR_{H2} is found in the parietal cell in the stomach, and both broxyquinoline and chloroxine can be found in the gastrointestinal tract at currently prescribed dosages. Chloroxine is used as an antidiarrhea medication in the treatment of intestinal microflora disorders, with a dosage of 250 mg, resulting in a theoretical maximum stomach concentration of 1.2 mM, more than 100 times the functional concentration shown here. Broxyquinoline (Intestopan) is an antiprotozooan and also used to treat diarrhea and inhibit cryptosporidium growth.[28] Broxyquinoline dosage is two 500 mg capsules, given three times a day.[29] If all broxyquinoline makes it to the stomach to interact with HR_{H2} expressing parietal cells, the receptors could experience broxyquinoline concentrations of up to 3.3 mM, more than 300 times the functional concentration shown here.

CONCLUSIONS

Taken together, HR_{H2} and GPR119 successfully coupled to the yeast machinery to generate high-throughput sensors. We use the HR_{H2}-based sensor in yeast to screen a 403-member anti-infection library leading to the discovery of chlorquinaldol, chloroxine, and broxyquinoline as HR_{H2} blockers in yeast. We show that 8-hydroxyquinoline is a general HR_{H2} blocker scaffold, and via computational docking studies using an HR_{H2} model, we put forth that 8-hydroxyquinoline binds at the same site as histamine, albeit making electrostatic contacts with Asp186 and Thr190 rather than Asp98 and Tyr250. Preliminary structure–activity relationship (SAR) studies suggest that the identified 8-hydroxyquinoline HR_{H2} blockers are competitive agonists, with potentially a different type of agonist behavior based on the moiety at the C_2 position. Future mutagenesis studies are needed to confirm the role of Asp186 and Thr190 in 8-hydroxyquinoline binding as well as confirm the HR_{H2} antagonism mechanism.

As the blockers were discovered using a synthetic yeast assay, we validated the HR_{H2} blocker hits in mammalian cells, establishing 8-hydroxyquinoline as a new scaffold of HR_{H2} blockers. This sets the stage for using the 8-hydroxyquinoline scaffold for the design of novel HR_{H2} therapeutics for the treatment of acid reflux without the cancer-causing moiety present on many current HR_{H2} blockers. Of note, the three HR_{H2} blockers identified in this work are antimicrobials. Broxyquinoline and chloroxine can be found in the gut at concentrations that block HR_{H2} at currently prescribed concentrations. Chlorquinaldol (Siosteran) is a topical antimicrobial agent.[30] The identification of antimicrobial-gut GPCR interactions shows that antimicrobials interact with

https://doi.org/10.1021/acssynbio.2c00205
ACS Synth. Biol. 2022, 11, 2820–2828

human receptors and their activity in the gut may not be confined to only interactions with the microbiota.

METHODS

Materials. The anti-infection chemical library (L3100) was purchased from Selleck Chemicals. Luciferase expression was assayed using the NanoGlo Luciferase Assay System (Promega N1120). Histamine dihydrochloride (Sigma H7250), famotidine (TCI F0530), oleolyethanolamide (Cayman 90265), lithocholic acid (Cayman 20253), chlorquinaldol (Selleck S4192), chloroxine (Selleck S1839), and broxyquinoline (Selleck S4195) were purchased from the specified vendors. HEK293T cells (CRL-11268) were obtained from ATCC.

G_s-Coupled GPCR-Based Sensor Construction. HR_{H2} (Uniprot P2501), GPR119 (Uniprot Q8TDV5), and GPBAR1 (Uniprot Q8TDU6) were codon-optimized for *S. cerevisiae*, commercially synthesized (Thermo Fisher), and cloned into pESC-HIS3-P_{TEF}-P_{ADH} (pKM111)[10] at *Bam*HI/*Sac*II to generate pESC-HIS3-P_{TEF}-HR_{H2} (pRLH16), pESC-HIS3-P_{TEF}-GPR119 (pRLH15), and pESC-HIS3-P_{TEF}-GPBAR1 (pRLH14), respectively. Constructs were sequence verified using primers EY46−2/NK12. To generate the GPCR-based sensor strains, pRLH16, pRLH15, and pRLH14 were co-transformed with pRS415-Leu2-P_{FIG1}-NanoLuc (pEY15)[11] into PPY140 (*S. cerevisiae* W303 Δ*far1*, Δ*ste2*, Δ*sst2*)[10] to generate PPY2171, PPY2172, and PPY2173, respectively. The no receptor control strain (PPY1809) was generated via co-transformation of pEY15 and pKM111 into PPY140.[11]

Histamine, Oleoylethanolamide, and Lithocholic Acid Sensing. An overnight culture of PPY2171, PPY2172, PPY2173, or PPY1809 was used to inoculate 50 mL of synthetic complete medium with 2% glucose lacking histidine and leucine (SD(HL^-)) to an OD_{600} = 0.06. After 18 h at 15 °C (150 rpm), the cultures were centrifuged (3500 rpm, 10 min), and resuspended in SD(HL^-) to an OD_{600} = 1. In a white, flat-bottomed 96-well plate, 190 μL of pH 7 SD (HL^-), 8 μL of cells, and 2 μL of either histamine, oleoylethanolamide, or lithocholic acid (final concentration 0−10^4 μM), or DMSO as control were added. After chemical incubation (2.5 h, 30 °C, 250 rpm), 20 μL of a 1:100 mixture of NanoLuc substrate to NanoLuc buffer were added, and the reaction was incubated for 30 min (30 °C, 250 rpm). Luminescence was read in a Biotek Synergy 2 using default settings.

Screening 403-Member Anti-Infection Library for HR_{H2} Blockers. The histamine sensing protocol was followed except as described. In a white, flat-bottomed 96-well plate, 188 μL of pH 7 SD (HL^-), 8 μL of cells, 2 μL of histamine (final concentration of 100 μM), 2 μL of anti-infection library compound (final concentration of 1 μM) were added. For the no chemical control, only 4 μL of DMSO was added and no histamine or compound was added. False-positive identification: Dose−response curves of the 21 HR_{H2} blocker hits were performed by following the library screening protocol using 100 μM histamine and 0.1−100 μM HR_{H2} blocker hit.

HR_{H2} Blocker Hits Validation in Yeast. Dose−response curves were performed by following the library screening protocol using 1 mM histamine and 10^{-3}−10^2 μM of famotidine or the 7 HR_{H2} blocker hits. DMSO, the carrier solvent, was used as the no chemical control. The no receptor control strain was tested under the same conditions as the HR_{H2} sensor strain. The same protocol was used to validate cloxiquine, clioquinol, diiodohydroxyquinoline, and nitroxoline.

Yeast Toxicity Assay. To measure chloroxine, chlorquinaldol, and broxyquinoline toxicity to yeast, an overnight culture of PPY2171 was diluted to OD_{600} = 1 in fresh SD(HL^-). Histamine (10 μL, final concentration 1 mM) and HR_{H2} blocker hit (10 μL, final concentration 10^{-3}−10^2 μM) or DMSO as no chemical control was added to the cells. After chemical incubation (2.5 h, 30 °C, 250 rpm), absorbance (OD_{600}) was measured.

Docking of HR_{H2} Blockers in the HR_{H2} Model. The HR_{H2} structure was obtained from AlphaFold (UniProt P25021).[24,25] Structure data files for histamine (ZINC388081), chlorquinaldol (ZINC119403), chloroxine (ZINC1131), and broxyquinoline (ZINC1064) were obtained from the ZINC15 database.[31] Hydrogens were added using CACTUS structure file generator (https://cactus.nci.nih.gov/translate/), and ChemDraw was used to protonate the nitrogen in the imidazole ring of chlorquinaldol, chloroxine, and broxyquinoline. The grid box (binding pocket) was defined by Asp98, Asp186, and Thr190.[26] Each chemical was then docked using AutoDock 4.2.6 with results visualized in AutoDockTools1.5.7[32] and Pymol.

HR_{H2} Blocker Hits Validation in Mammalian Cells. HEK293T cells were grown in T75 flasks using growth medium (DMEM with GlutaMAX, 10% fetal bovine serum (FBS), and 1% pen/strep) at 37 °C with 5% CO_2 until reaching 70−90% confluence. Cells were harvested using 0.05% trypsin-EDTA and diluted to a concentration of 1.5 × 10^5 cells/mL. The cells were seeded into a 96-well plate (1.5 × 10^4 cells/well) and incubated overnight. The cells were transiently transfected with PPY2295 and PPY2325 using FuGENE HD (Promega), and the plate was incubated overnight. The following day, the growth media was replaced with freshly made equilibrium media (CO_2-independent medium with 10% FBS, and 5% GloSensor cAMP reagent). The plate was placed in the luminescent plate reader (BioTek Synergy 2), and the cells were equilibrated at 25 °C for 2 h with readings every 15 min. The plate was then removed, and 2 μL of famotidine, chloroxine, chlorquinaldol, or broxyquinoline (final concentration 0.1 μM to 1 mM) was added. As the no chemical control, 2 μL of DMSO was used. The plate was incubated for 10 min. Next, 2 μL of histamine (final concentration 1 μM) was added and the plate was placed back into the plate reader. Luminescence was read every 2 min for 30 min.

Mammalian Toxicity Assay. Mammalian cell viability was assayed using an MTT Cell Proliferation Assay Kit (Cayman Chemical, 10009365). HEK293T cells were cultured in T75 flasks until reaching 70−90% confluence. Cells were trypsinized, counted, and replated in a clear, flat-bottom 96-well plate at a concentration of 5 × 10^2 cells/well, and incubated overnight (37 °C with 5% CO_2). The cells were then incubated with 1 μm histamine and the HR_{H2} blocker hits (0.1 μM to 1 mM) or DMSO as a no chemical control. After 24 h, the directions from the MTT Assay Kit were followed. Briefly, 10 μL of MTT reagent was added to each well and the cells were incubated for 4 h. Next, 100 μL of crystal dissolving solution was added to each well and the cells were incubated for 18 h at 37 °C with 5% CO_2. Absorbance was read at 570 nm (BioTek Synergy 2) using default absorbance settings.

Determining HR_{H2}-Blocker Hit Mode of Action. The chemical library screening protocol was followed except that the HR_{H2}-based sensor was activated with histamine (10^{-2}−

https://doi.org/10.1021/acssynbio.2c00205
ACS Synth. Biol. 2022, 11, 2820−2828

10^3 μM) prior to the addition of chlorquinaldol, chloroxine, broxyquinoline, or famotidine (0, 1, 10, 50 nM).

Structural Characterization of Chlorquinaldol, Chloroxine, and Broxyquinoline. Chlorquinaldol: ^{1}H NMR (500 MHz, DMSO) δ 8.37 (dd, J = 8.6, 4.8 Hz, 1H), 7.73 (d, J = 3.9 Hz, 1H), 7.63 (dd, J = 8.7, 3.5 Hz, 1H), 2.76 (s, 3H). ^{13}C NMR (126 MHz, DMSO) δ 159.50, 148.91, 138.90, 133.28, 127.18, 124.53, 123.55, 119.51, 115.89, 25.06. Chloroxine: ^{1}H NMR (500 MHz, DMSO) δ 9.01 (dd, J = 4.2, 1.5 Hz, 1H), 8.53 (dd, J = 8.5, 1.5 Hz, 1H), 7.84 (s, 1H), 7.77 (dd, J = 8.5, 4.2 Hz, 1H). ^{13}C NMR (126 MHz, DMSO) δ 150.40, 149.74, 139.45, 133.39, 128.34, 125.32, 123.71, 119.39, 116.06. Broxyquinoline: ^{1}H NMR (500 MHz, DMSO) δ 8.98 (dd, J = 4.1, 1.5 Hz, 1H), 8.46 (dd, J = 8.6, 1.5 Hz, 1H), 8.08 (s, 1H), 7.79 (dd, J = 8.5, 4.2 Hz, 1H). ^{13}C NMR (126 MHz, DMSO) δ 151.57, 150.34, 139.44, 135.93, 133.77, 126.97, 124.18, 109.29, 105.60.

■ ASSOCIATED CONTENT

Supporting Information

The Supporting Information is available free of charge at https://pubs.acs.org/doi/10.1021/acssynbio.2c00205.

Plasmids (Supporting Table 1); strains (Supporting Table 2); primers (Supporting Table 3); response of the GPBAR1-based sensor to lithocholic acid (Supporting Figure 1); patch screen of HR_{H2}-based, GPR119-based, and GPBAR1-based yeast biosensors (Supporting Figure 2); dose−response curve of HR_{H2} sensor with tioconazole (Supporting Figure 3); dose−response curves of HR_{H2}-based sensor with the 21 HR_{H2} blocker hits (Supporting Figure 4); dose−response curves of closantel, octenidine, cetylpyridinium, and enroflaxacin (Supporting Figure 5); dose−response curves of HEK293T cells co-transfected with HR_{H2} and cAMP sensor in the presence of histamine, chlorquinaldol, chloroxine, and broxyquinoline (Supporting Figure 6); ^{1}H-NMR chlorquinaldol (Supporting Figure 7); ^{13}C-NMR chlorquinaldol (Supporting Figure 8;) ^{1}H-NMR chloroxine (Supporting Figure 9); ^{13}C-NMR chloroxine (Supporting Figure 10); ^{1}H-NMR broxyquinoline (Supporting Figure 11); ^{13}C-NMR broxyquinoline sequences (Supporting Figure 12); Sequences; and References (PDF)

■ AUTHOR INFORMATION

Corresponding Author

Pamela Peralta-Yahya − *School of Chemistry and Biochemistry, Georgia Institute of Technology, Atlanta, Georgia 30332, United States; School of Chemical & Biomolecular Engineering, Georgia Institute of Technology, Atlanta, Georgia 30332, United States;* orcid.org/0000-0002-0356-2274; Email: pperalta-yahya@chemistry.gatech.edu

Authors

Paola L. Marquez-Gomez − *School of Chemistry and Biochemistry, Georgia Institute of Technology, Atlanta, Georgia 30332, United States*

Nicholas S. Kruyer − *School of Chemical & Biomolecular Engineering, Georgia Institute of Technology, Atlanta, Georgia 30332, United States*

Sara L. Eisen − *School of Chemistry and Biochemistry, Georgia Institute of Technology, Atlanta, Georgia 30332, United States*

Lily R. Torp − *School of Chemistry and Biochemistry, Georgia Institute of Technology, Atlanta, Georgia 30332, United States*

Rebecca L. Howie − *School of Chemistry and Biochemistry, Georgia Institute of Technology, Atlanta, Georgia 30332, United States*

Elizabeth V. Jones − *School of Chemistry and Biochemistry, Georgia Institute of Technology, Atlanta, Georgia 30332, United States*

Stefan France − *School of Chemistry and Biochemistry, Georgia Institute of Technology, Atlanta, Georgia 30332, United States;* orcid.org/0000-0001-5998-6167

Complete contact information is available at: https://pubs.acs.org/10.1021/acssynbio.2c00205

Author Contributions

[§]P.L.M.-G. and N.S.K. contributed equally to this work. P.L.M.-G, N.S.K., S.L.E., L.R.T., and R.L.H. designed the research, performed the experiments, and analyzed the data. E.V.J. collected and analyzed the NMR data of chlorquinaldol, chloroxine, and broxyquinoline. P.P.-Y. designed the research and analyzed the data. P.P.-Y. and N.S.K. wrote the manuscript.

Notes

The authors declare no competing financial interest.

■ ACKNOWLEDGMENTS

Research reported in this publication was supported by the National Institute of General Medical Sciences of the National Institutes of Health under Award Number R35GM124871. The content is solely the responsibility of the authors and does not necessarily represent the official views of the National Institutes of Health.

■ ABBREVIATIONS

cAMP, cyclic adenosine monophosphate; HEK293T, human embryonic kidney cells; GPCR, G-protein-coupled receptor; HR_{H2}, histamine receptor 2

■ REFERENCES

(1) Samuelson, L. C.; Hinkle, K. L. Insights into the regulation of gastric acid secretion through analysis of genetically engineered mice. *Annu. Rev. Physiol.* **2003**, *65*, 383−400.

(2) Almario, C. V.; Ballal, M. L.; Chey, W. D.; Nordstrom, C.; Khanna, D.; Spiegel, B.M.R. Burden of gastrointestinal symptoms in the United States: results of a nationally representative survey of over 71,000 Americans. *Am. J. Gastroenterol.* **2018**, *113*, 1701−1710.

(3) El-Serag, H. B.; Sweet, S.; Winchester, C. C.; Dent, J. Update on the epidemiology of gastro-oesophageal reflux disease: a systematic review. *Gut* **2014**, *63*, 871−880.

(4) Le Roux, J.; Gallard, H.; Croue, J. P. Formation of NDMA and halogenated DBPs by chloramination of tertiary amines: the influence of bromide ion. *Environ. Sci. Technol.* **2012**, *46*, 1581−1589.

(5) White, C. M. Ranitidine's *N*-nitrosodimethylamine Problem May be Tip of the Iceberg. *JAMA Netw Open.* **2021**, *4*, No. e2035158.

(6) FDA News Release, FDA Requests removal of all ranitidine products (Zantac) from the market, April 01, 2020. https://www.fda.gov/news-events/press-announcements/fda-requests-removal-all-ranitidine-products-zantac-market.

(7) Walker, M.J.A. The major impacts of James Black's drug discoveries on medicine and pharmacology. *Trends Pharmacol. Sci.* **2011**, *32*, 183−188.
(8) Yasi, E. A.; Kruyer, N. S.; Peralta-Yahya, P. Advances in G protein-coupled receptor high-throughput screening. *Curr. Opin. Biotechnol.* **2020**, *64*, 210−217.
(9) Saitoh, T.; Fukushima, Y.; Otsuka, H.; Ishikawa, M.; Tamai, M.; Takahashi, H.; Mori, H.; Asano, T.; Anai, M.; Ishikawa, T.; Katsube, T.; Ogawa, K.; Kajiwara, T.; Omata, M.; Ohkawa, S. Effects of N-alpha-methyl-histamine on human H_2 receptors expressed in CHO cells. *Gut* **2002**, *50*, 786−789.
(10) Shi, Z.; Fultz, R. S.; Engevik, M. A.; Gao, C.; Hall, A.; Major, A.; Mori-Akiyama, Y.; Versalovic, J. Distinct roles of histamine H_1- and H_2-receptor signaling pathways in inflammation-associated colonic tumorigenesis. *Am. J. Physiol.: Gastrointest. Liver Physiol.* **2019**, *316*, G205−G216.
(11) Mukherjee, K.; Bhattacharyya, S.; Peralta-Yahya, P. GPCR-based chemical biosensors for medium-chain fatty acids. *ACS Synth. Biol.* **2015**, *4*, 1261−1269.
(12) Yasi, E. A.; Allen, A. A.; Sugianto, W.; Peralta-Yahya, P. Identification of three antimicrobials activating serotonin receptor 4 in colon cells. *ACS Synth. Biol.* **2019**, *8*, 2710−2717.
(13) Yasi, E. A.; Eisen, S. L.; Wang, H.; Sugianto, W.; Minniefield, A. R.; Hoover, K. A.; Branham, P. J.; Peralta-Yahya, P. Rapid deorphanization of human olfactory receptors in yeast. *Biochemistry* **2019**, *58*, 2160−2166.
(14) Ehrenworth, A. M.; Claiborne, T.; Peralta-Yahya, P. Medium-throughput screen of microbially produced serotonin via a G-protein-coupled receptor-based sensor. *Biochemistry* **2017**, *56*, 5471−5475.
(15) Okashah, N.; Wan, Q.; Ghosh, S.; Sandhu, M.; Inoue, A.; Vaidehi, N.; Lambert, N. A. Variable G protein determinants of GPCR coupling selectivity. *Proc. Natl. Acad. Sci. U.S.A.* **2019**, *116*, 12054.
(16) Ritter, K.; Buning, C.; Halland, N.; Pöverlein, C.; Schwink, L. G protein-coupled receptor 119 (GPR119) agonists for the treatment of diabetes: recent progress and prevailing challenges. *J. Med. Chem.* **2016**, *59*, 3579−3592.
(17) Overton, H. A.; Babbs, A. J.; Doel, S. M.; Fyfe, M. C.; Gardner, L. S.; Griffin, G.; Jackson, H. C.; Procter, M. J.; Rasamison, C. M.; Tang-Christensen, M.; Widdowson, P. S.; Williams, G. M.; Reynet, C. Deorphanization of a G protein-coupled receptor for oleoylethanolamide and its use in the discovery of small-molecule hypophagic agents. *Cell Metab.* **2006**, *3*, 167−175.
(18) Biagioli, M.; Carino, A.; Cipriani, S.; Francisci, D.; Marchianò, S.; Scarpelli, P.; Sorcini, D.; Zampella, A.; Fiorucci, S. The bile acid receptor GPBAR1 regulates the M1/M2 phenotype of intestinal macrophages and activation of GPCAR1 rescues mice from murine colitis. *J. Immunol.* **2017**, *199*, 718−733.
(19) Luo, M.; Zhou, W.; Patel, H.; Srivastava, A. P.; Symersky, J.; Bonar, M. M.; Faraldo-Gómez, J. D.; Liao, M.; Mueller, D. M. Bedaquiline inhibits the yeast and human mitochondrial ATP synthases. *Commun. Biol.* **2020**, *3*, No. 452.
(20) Hrenovic, J.; Ivankovic, T.; Sekovanic, L.; Rozic, M. Toxicity of dodecylpyridiniuim and cetylpyridinium clorides against phosphate-accumulating bacterium. *Open Life Sci.* **2008**, *3*, 143−148.
(21) Ellabib, M.; Ghannoum, M. A.; Whittaker, P. A. Effects of the pyridinamines octenidine and pirtenidine on yeast mitochondrial function. *Biochem. Soc. Trans.* **1990**, *18*, 342−343.
(22) Gaulton, A.; Hersey, A.; Nowotka, M.; Bento, A. P.; Chambers, J.; Mendez, D.; Mutowo, P.; Atkinson, F.; Bellis, L. J.; Cibrián-Uhalte, E.; Davies, M.; Dedman, N.; Karlsson, A.; Magariños, M. P.; Overington, J. P.; Papadatos, G.; Smit, I.; Leach, A. R. The ChEMBL database in 2017. *Nucleic Acids Res.* **2017**, *45*, D945−D954.
(23) Vass, M.; Podlewska, S.; de Esch, I.J.P.; Bojarski, A. J.; Leurs, R.; Kooistra, A. J.; de Graaf, C. Aminergic GPCR-Ligand Interactions: A Chemical and Structural Map of Receptor Mutation Data. *J. Med. Chem.* **2019**, *62*, 3784−3839.
(24) Jumper, J.; Evans, R.; Pritzel, A.; Green, T.; Figurnov, M.; Ronneberger, O.; Tunyasuvunakool, K.; Bates, R.; Žídek, A.; Potapenko, A.; Bridgland, A.; Meyer, C.; Kohl, SAA.; Ballard, A. J.; Cowie, A.; Romera-Paredes, B.; Nikolov, S.; Jain, R.; Adler, J.; Back, T.; Petersen, S.; Reiman, D.; Clancy, E.; Zielinski, M.; Steinegger, M.; Pacholska, M.; Berghammer, T.; Bodenstein, S.; Silver, D.; Vinyals, O.; Senior, A. W.; Kavukcuoglu, K.; Kohli, P.; Hassabis, D. Highly accurate protein structure prediction with AlphaFold. *Nature* **2021**, *596*, 583−589.
(25) Varadi, M.; Anyango, S.; Deshpande, M.; Nair, S.; Natassia, C.; Yordanova, G.; Yuan, D.; Stroe, O.; Wood, G.; Laydon, A.; Žídek, A.; Green, T.; Tunyasuvunakool, K.; Petersen, S.; Jumper, J.; Clancy, E.; Green, R.; Vora, A.; Lutfi, M.; Figurnov, M.; Cowie, A.; Hobbs, N.; Kohli, P.; Kleywegt, G.; Birney, E.; Hassabis, D.; Velankar, S. AlphaFold protein structure database: massively expanding the structural coverage of protein-sequence space with high-accuracy models. *Nucleic Acids Res.* **2022**, *50*, D439−D444.
(26) Gantz, I.; DelValle, J.; Wang, L. D.; Tashiro, T.; Munzert, G.; Guo, Y. J.; Konda, Y.; Yamada, T. Molecular basis for the interaction of histamine with the histamine H2 receptor. *J. Biol. Chem.* **1992**, *267*, 20840−20843.
(27) Sun, X.; Li, Y.; Li, W.; Xu, Z.; Tang, Y. Computational investigation of interactions between human H2 receptors and its agonists. *J. Mol. Graphics Modell.* **2011**, *29*, 693−701.
(28) Fritzler, J. M.; Zhu, G. Novel anti-cryptosporidium activity of known drugs identified by high-throughput screening against parasite fatty acyl-CoA binding protein (ACBP). *J. Antimicrob. Chemother.* **2012**, *67*, 609−617.
(29) Swain, R.; Bapna, J. S.; Das, A. K.; Chandrasekar, S.; Swaminathan, R. P.; Bosco, B.; Veliath, S.; Thombre, D. P. A study on the neurotoxicity of broxyquinoline and brobenzoxaldine combination in therapeutic doses. *Human Toxicol.* **1986**, *5*, 35−41.
(30) Bidossi, A.; Bottagisio, M.; De Grandi, R.; Drago, L.; De Vecchi, E. Chlorquinaldol, a topical agent for skin and wound infections: anti-biofilm activity and biofilm-related antimicrobial cross-resistance. *Infect. Drug Resist* **2019**, *12*, 2177−2189.
(31) Sterling, T.; Irwin, J. J. ZINC15 − Ligand discovery for everyone. *J. Chem. Inf. Model* **2015**, *55*, 2324−2337.
(32) Morris, G. M.; Huey, R.; Lindstrom, W.; Sanner, M. F.; Belew, R. K.; Goodsell, D. S.; Olson, A. J. Autodock4 and AutoDockTools4: automated docking with selective receptor flexiblity. *J. Comput. Chem.* **2009**, *30*, 2785−2791.

https://doi.org/10.1021/acssynbio.2c00205
ACS Synth. Biol. 2022, 11, 2820−2828